Measurement of the internal impedance of traction rails at 50 Hz

Andrea Mariscotti, P. Pozzobon

To cite this version:

Andrea Mariscotti, P. Pozzobon. Measurement of the internal impedance of traction rails at 50 Hz. IEEE Transactions on Instrumentation and Measurement, 2000, 49 (2), pp.294-299. 10.1109/19.843067 . hal-02970378

HAL Id: hal-02970378
https://hal.science/hal-02970378

Submitted on 18 Oct 2020

HAL is a multi-disciplinary open access archive for the deposit and dissemination of scientific research documents, whether they are published or not. The documents may come from teaching and research institutions in France or abroad, or from public or private research centers.

L'archive ouverte pluridisciplinaire **HAL**, est destinée au dépôt et à la diffusion de documents scientifiques de niveau recherche, publiés ou non, émanant des établissements d'enseignement et de recherche français ou étrangers, des laboratoires publics ou privés.

Measurement of the Internal Impedance of Traction Rails at 50 Hz

A. Mariscotti, P. Pozzobon

Dipartimento di Ingegneria Elettrica, Via dell’Opera Pia, 11A – 16145 Genova – Italy

A. Mariscotti and P. Pozzobon, “Measurement of the Internal Impedance of Traction Rails at 50 Hz,” *IEEE Transactions on Instrumentation and Measurement*, Vol.49, No. 2, April 2000, pp. 294-299. doi: 10.1109/19.843067.

Abstract

The electrical behaviour of sample steel traction rails is analysed considering the resistance and the external and internal inductance. Measurements are performed on two rails arrangements at different current levels (up to nearly 2 kA) at 50 Hz and over an extended frequency range (50 Hz to 100 kHz) at low currents, so that skin effect and saturation phenomena are clearly visible. Great accordance with the results obtained using Carson's formulae is found.

Keywords

Electric variables measurement, Time measurement, Inductance measurement, Resistance measurement, Frequency measurement, Frequency measurement, Rail transportation power systems

1. Introduction

The rails are one of the most important elements of a railway system from the electrical point of view: they are the electrical interface between first, the traction circuit and the signalling circuits and second, the traction circuit and the ground reference circuit.

Signalling circuits like track circuits use the rails as a part of the transmitter-receiver circuit and include rail inductance in the calculations of the resonance frequency of the tuned circuits used for jointless separation of rail sections. Hence, it is very important to know the per-unit-length rails inductance and also its dependence on frequency and current. Moreover, the traction return current from locomotives divides among the ground and the rails, highly depending on their longitudinal parameters, exposing signalling circuits to the threat of electromagnetic interference.

Measurements should be taken, if possible, not only on rail material samples but also on rail pieces used in railways for normal service, exposed to ageing, mechanical stresses and return traction current magnetisation.

Rails are almost always considered as a structural element of the railway system and attention is focused on mechanical characteristics; so, information on electrical characteristics is generally limited to dc resistance (and 16.7 or 50 Hz reactance in some cases).

Few previous works [1,2,3,4] (spanning over 80 years) analysed the electrical behaviour of rails in different circuit arrangements and under different operating conditions (frequency and current).

2. Rail resistance and inductance (low current tests)

The test circuit is a loop circuit with the rails shorted at the far end and supplied in differential mode (Fig. 1).

Rails characteristics are reported in Table I.

A preliminary estimation of the rail resistance has been made in order to define an upper limit of the resistance of the cables, connectors and short circuit connection: assuming a steel resistivity of 0.22 Ω mm^2/m, it is obtained $R_{dc,appr.}$=28.6 μΩ/m, with an expected variation of 2-3 orders of magnitude (due to skin effect) for frequencies ranging from 50 Hz to 100 kHz.

The characteristics of the four contacts at the rails terminals and of the supply and short cables (connected to the rails ends) are reported in Table II; one assembled rail input terminal is shown in Fig. 2.

Carson's formulae [5,6] are used as a reference to evaluate circuit resistance and inductance; the latter must be considered contributed by two terms: internal (L_{int}) and external (L_{ext}) inductance.

Three assumptions are generally made:

- conductors of infinite length;
- parallel conductors;
- return ground homogeneous and of constant resistivity.

The external self impedance is

$$Z_{ii,ext} = j\omega \frac{\mu_0}{2\pi} \ln \frac{2h_i}{r_i} + 2\left(\Delta R_{ii} + j\Delta X_{ii}\right)$$

and the mutual impedance is

$$Z_{ij,ext} = j\omega \frac{\mu_0}{2\pi} \ln \frac{D_{ij}}{d_{ij}} + 2\left(\Delta R_{ij} + j\Delta X_{ij}\right)$$

where:

d_{ij} is the distance between conductors *i* and *j*;

D_{ij} is the distance between conductor *i* and image of conductor *j*, and vice versa;

h_i is the height above ground of conductor i;

r_i is the radius of conductor i.

The expressions of the corrective terms ΔR_{ii}, ΔR_{ij}, ΔX_{ii}, ΔX_{ij} may be found in [5,6].

A Thomson bridge method was adopted (see Fig. 3) to measure contacts resistance, using a sensitive galvanometer and 12 V battery as dc current source: the current flowing into the circuit is measured with a precision series resistor.

Results of the measurements performed on all the four terminals are shown in Table III.

From the comparison of the inductance and resistance values derived from Carson's formulae and the measurement results, it was immediately clear that:

- the feeding cables contribute a nearly constant inductance term (external inductance) and variable resistance term (skin effect at high frequencies);
- the contact resistance must be included to get more precise results for the resistance at low frequencies.

The cables inductance term was then hand calculated [7] (approx. = 3.9 μH) and it was found in accordance with the value corresponding to the constant difference between the two curves of Fig. 4(a).

Observing Fig. 4(a), the experimental points seem to diverge from the solid curve at low frequency (especially at 50 Hz); it was evident that the RLC automatic bridge is quite sensitive to the 50 Hz component and also to the harmonic components of the supply voltage (as it is shown after in Fig. 9).

The relative error is very small, especially in the most important frequency interval (from some hundred Hz up to some tens of kHz), where the large part of railway and metro signalling systems operate.

For the resistance term an accurate calculation was performed, considering both lumped and distributed models of the rails circuit. The distributed model is used to include capacitances and conductances at high frequency in the calculation (see Fig. 6).

The error curve for the rail resistance has higher values, but observing that the curve oscillates around small values (Fig. 6(b)), it may be stated that a large part of the error is contributed by the connections (resistance of the contacts with respect to that of rails) and by the accuracy of the measuring equipment.

Significant improvement will come from much longer sample rails, which in turn imply problems regarding the size and rated power of the measuring system.

3. Rail resistance and inductance (High current tests)

Test have been performed only at 50 Hz, where very high current amplitudes were available. Resistance and inductance are treated as the real and imaginary part of the measured impedance (voltamperometric method). Again, the resistance and inductance of the supply system (cables and contacts) were considered; the values calculated in the preceding section are subtracted from all readings.

Currents are measured by means of Hall effect sensors connected to a storage digital oscilloscope (see Fig. 7).

The Hall effect sensors were characterised using a precision Current Transformer for laboratory use.

The characteristics of the HFA1C300 and HA400R sensors are briefly reported in Table IV.

3.1 Rail-to-rail separation 1.5 m

Resistance and inductance of circuit components were preliminarily computed to determine approximately voltage and current ratings.

The measuring system for low output voltage is shown in Fig. 8; for high output voltage the single phase autotransformer is eliminated from the circuit.

The input autotransformer is supplied from the line-to-line voltage (380 Vrms), where the odd harmonics multiple of three are negligible. The Individual Harmonic Distortion (IHD) and Total Harmonic Distortion (THD) of the applied voltage are reported in Fig. 9.

Measurements were performed at 18 different current values; these are reported in Table V, where the rms values of the current flowing into the rails are shown.

The resistance and the internal inductance are plotted in the following figures as a function of the rail current.

The internal inductance is computed from the total measured inductance subtracting the contribution of the external inductance, which was estimated using the 100 kHz reading of the low current tests (see section II); at this frequency it may be assumed that the total inductance was contributed exclusively by the circuit geometry (external inductance).

For ease of comparison resistance and inductance are shown in per-unit-length values.

The resistance and internal inductance have been interpolated using 3rd and 4th order polynomials respectively with Least Mean Squares algorithm.

$$R = -4.37\,10^{-14} I^3 - 3.36\,10^{-11} I^2 + 2.71\,10^{-7} I + 7.05\,10^{-5}$$

$$L_{\mathrm{int}} = 3.94\,10^{-19} I^4 - 1.03\,10^{-15} I^3 - 3.39\,10^{-13} I^2 + \\ + 6.32\,10^{-10} I + 4.07\,10^{-8}$$

The resistance and inductance curves of Fig. 10 suggest that in the interval 800–1000 A saturation occurs. This will be confirmed by the high current measurements shown hereafter.

3.2 Rail-to-rail separation 0.5 m

Higher currents are attained reducing the distance between rails to 0.5 m, in order to reduce the external inductance and hence circuit impedance. Hall sensors cannot be used (because of maximum current limitation) and a Current Transformer (Hartmann&Braun) was chosen, connected to a precision load resistor. The cross section of the feeding cable from the transformer secondary winding was doubled from 150 to 300 mm^2.

Measurements were performed at 14 different current values; these are reported in Table VI, where the rms values of the current flowing into the rails are shown.

The resistance and the internal inductance are plotted in Fig. 11 as a function of the rail current.

For ease of comparison resistance and inductance are shown in per-unit-length values.

The resistance and internal inductance have been interpolated using 3rd and 4th order polynomials respectively with Least Mean Squares algorithm.

$$R = -8.31\,10^{-15} I^3 - 3.71\,10^{-11} I^2 + 5.2\,10^{-8} I + 4.9\,10^{-7}$$

$$L_{\mathrm{int}} = -7.55\,10^{-20} I^4 + 4.89\,10^{-16} I^3 - \\ - 1.16\,10^{-12} I^2 + 1.1\,10^{-9} I - 3.84\,10^{-8}$$

4. Conclusions

Electrical properties of traction rails (resistance and inductance) have been investigated at low and high currents both at 50 Hz and at higher frequency. The measuring system has been described, considering also limitations of the feeding and measuring devices and equipments. The results are in accordance with the values predicted by Carson formulae [5]. The measurement results have in turn increased the authors' confidence in using Carson formulae even for extreme cases (the conductors are short and quite near to the ground). The reported results are also a basis for the evaluation of the electrical behaviour of the rails at high currents during normal operation inside a railway system.

Future work will be the analysis of rail behaviour at high frequency (from some kHz up to some MHz), when they are biased by the traction return current (either dc or 50 Hz).

5. References

[1] E. Kennelli, F.H. Achard, S. Dana “Experimental researches on the skin effect in steel rails“, Journal of the Franklin Institute, Aug. 1916

[2] H.M. Trueblood, G. Wascheck “Investigation of rail impedances“, Electrical Engineering, 1933, pp. 898–907

[3] R.J. Hill, D.C. Carpenter “Determination of rail internal impedence for electric railway traction system simulation”, IEE Proc. part B, Vol. 138, n. 6, Nov. 1991

[4] J.C. Brown, J. Allan, B. Mellit “Calculation and measurement of rail impedances applicable to remote short circuit fault currents”, IEE Proc. part B, Vol.139, n.4, July 1992

[5] CCITT Directive *Vol. II – Calculating induced voltages and currents in practical cases*, Geneva, 1989

[6] J.R. Carson “Wave propagation in overhead wires with ground return“, Bell Systems Technical Journal, October 1926, vol. 5, pp. 539-554

[7] E.B. Rosa, F.W. Grover “Formulas and tables for the calculations of mutual and self inductance“, Scientific papers of Bureau of Standards, n. 169, Washington, 1948

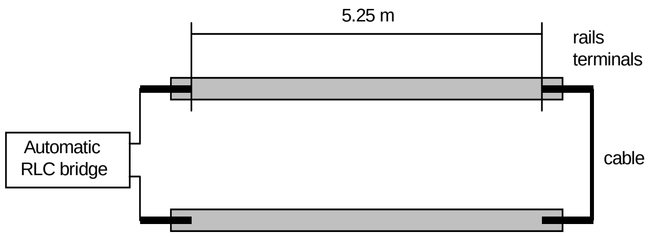

Figure 1: Measuring circuit for low current tests

TABLE I
RAIL CHARACTERISTICS

Type	UNI 60
Section [mm^2]	7679
Length [m]	5.8

TABLE II
CONTACTS AND CABLES CHARACTERISTICS

Copper bars with 5×50 mm^2 and 10×50 mm^2 cross sections
Silver coated surfaces

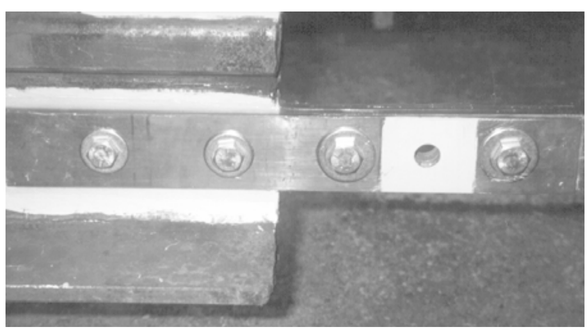

Figure 2: Arrangement of rail feeding terminals

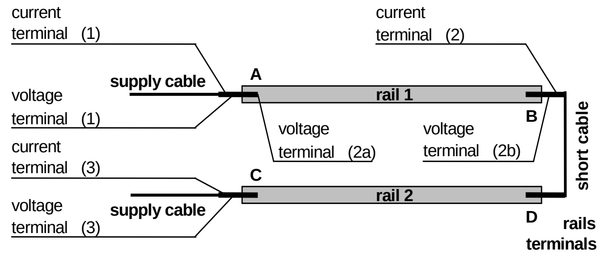

Figure 3: Configurations of voltamperometric measurements of the dc resistance of contacts and rails

TABLE III
MEASURED DC RESISTANCE OF CONTACTS AND RAILS

R_A	0.092 mΩ	R_C	0.1085 mΩ
R_B	0.1148 mΩ	$R_{D+sh.cable}$	0.1335 mΩ
R_{rail1}	0.3542 mΩ	R_{rail2}	0.35 mΩ
$R_{total,A-C}$	1.153 mΩ		

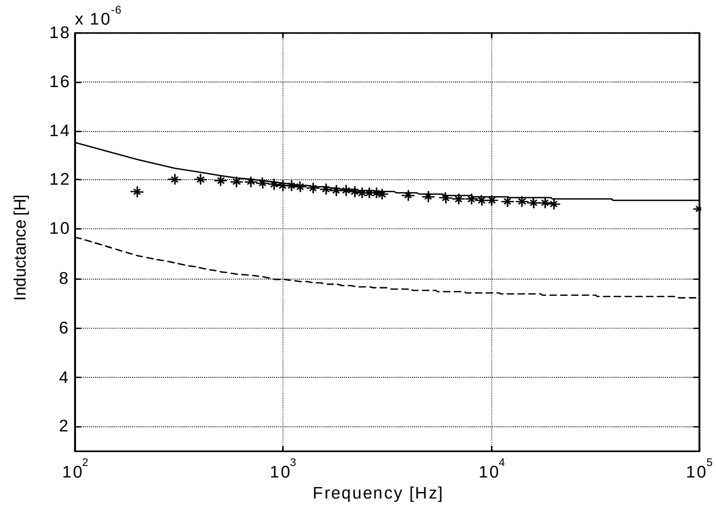

(a)

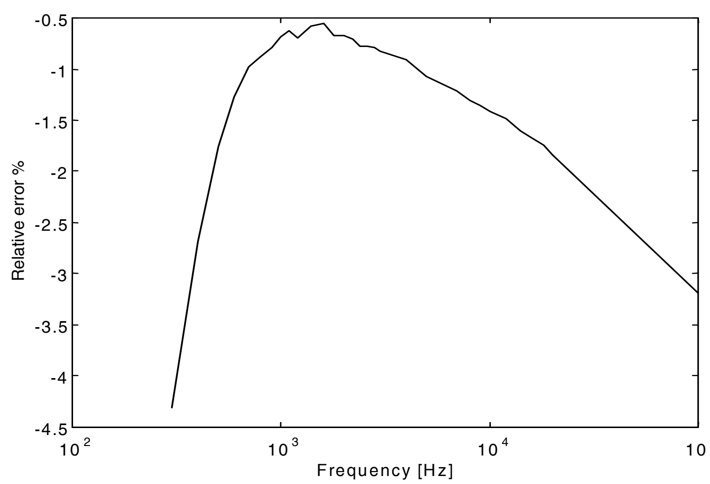

(b)

Figure 4: Rails inductance vs. frequency (low current):

(a) theoretical (— with and – – – without cables inductance) and experimental ($*$); (b) relative error

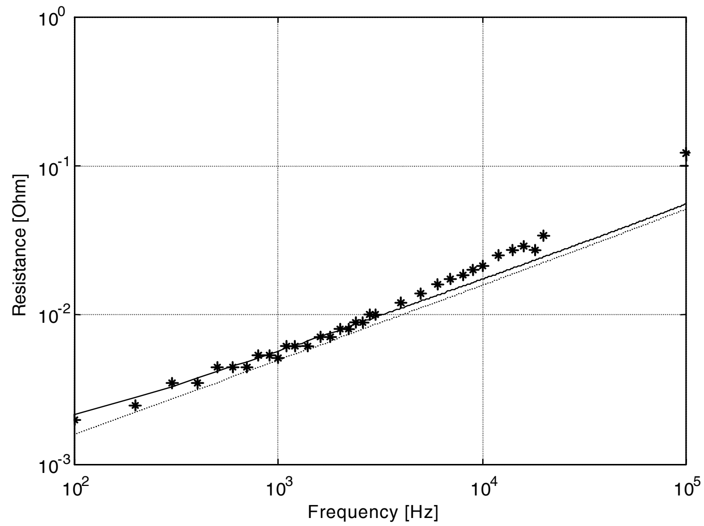

(a)

Figure 5: Rails resistance vs. frequency (low current test and lumped parameters model): theoretical (— with and – – – without cables and contacts resistance) and experimental ($*$)

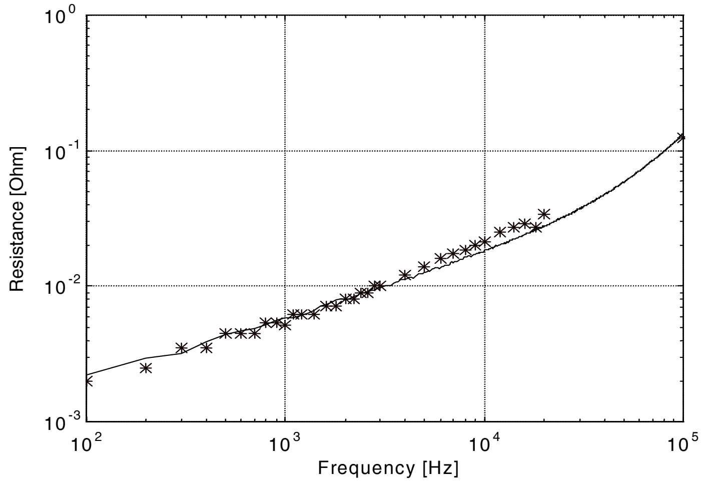

(a)

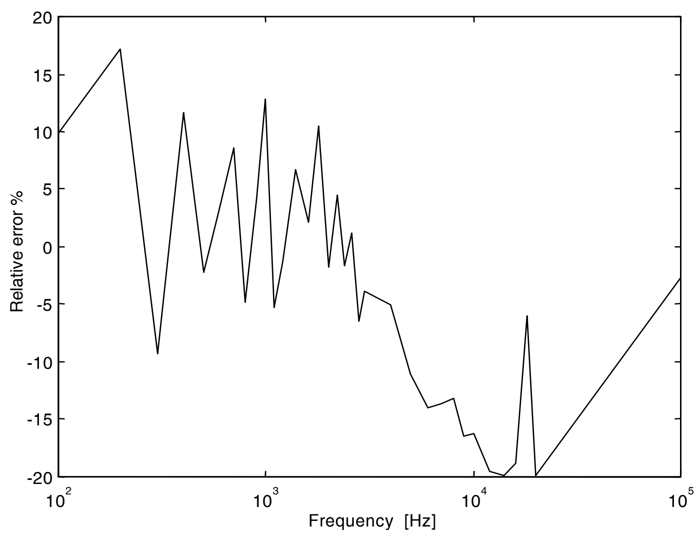

(b)

Figure 6: Rails resistance vs. frequency (low current test and distributed parameters model): (a) theoretical (—) and experimental ($*$); (b) relative error

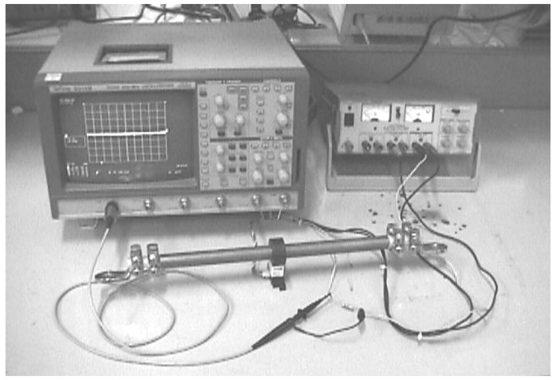

Figure 7: Hall effect sensor HFA1C300 (on the copper bar); power supply; digital oscilloscope LeCroy 9314M

TABLE IV
CHARACTERISTICS OF THE HALL EFFECT SENSORS

Parameter	**HA400R**	**HFA1C300**
Rated current	400 A	300 A
Saturation current	900 A	450 A
Output voltage	4 V ±1%	4 V (27Ω load)
Output current		150mA ±2% f.s.
Bandwidth	0÷10kHz	0÷200kHz

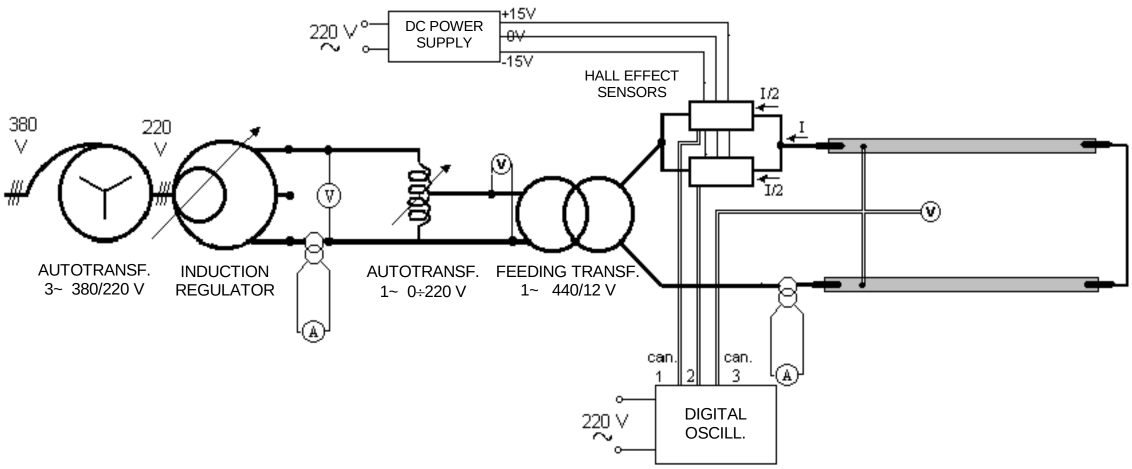

Figure 8: Measuring system for high current tests

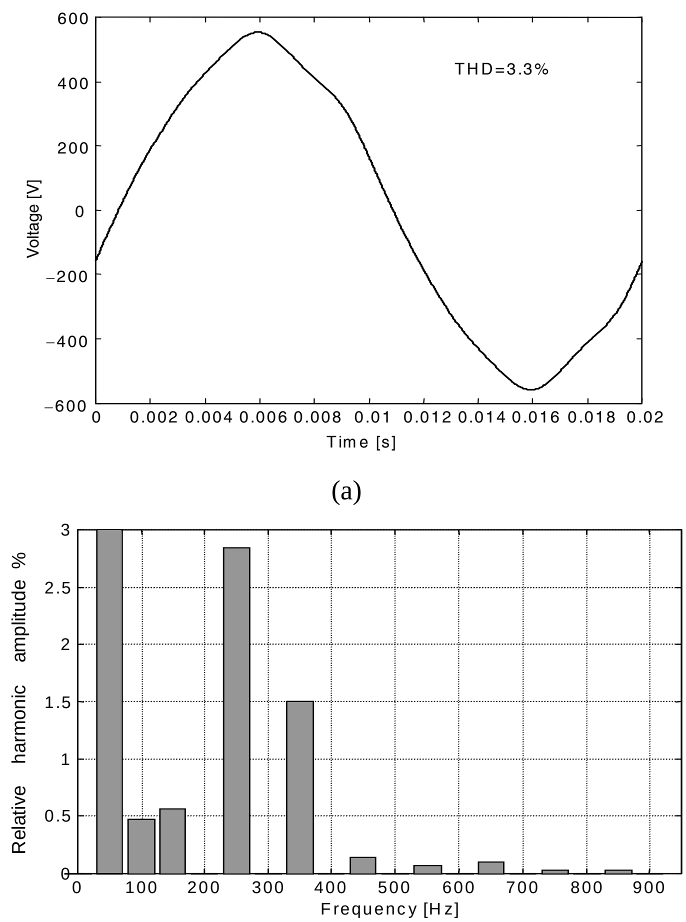

(a)

(b)

Figure 9: Line-to-line voltage (a) waveform and (b) harmonic spectrum

TABLE V

RESULTS FOR 1.5 METRES RAILS SEPARATION

Irms [A]	**R_{rail} [mΩ]**	**L_{tot} [μH]**	**L_{int} [μH]**
60.6	1.1	11.51	0.71
126.8	1.1	11.96	1.16
153.4	1.0	12.32	1.52
204.7	1.1	12.88	2.08
258.2	1.3	12.95	2.15
311.0	1.6	13.26	2.46
355.6	1.8	13.64	2.84
412.8	2.0	13.67	2.87
460.3	2.1	14.16	3.36
514.1	2.2	14.40	3.60
582.3	2.1	14.47	3.68
644.0	2.2	15.01	4.21
737.2	2.4	15.12	4.32
845.6	2.6	14.76	3.96
947.4	2.8	14.94	4.14
1041.0	2.9	14.78	3.98
1174.0	2.9	14.05	3.25
1258.1	2.8	14.06	3.26

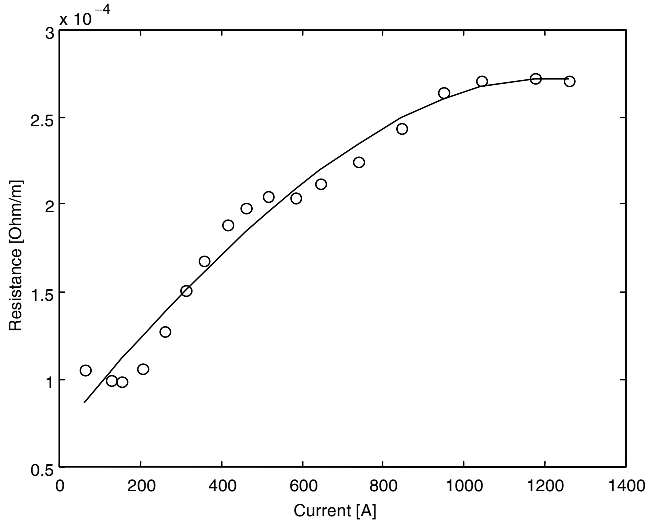

(a)

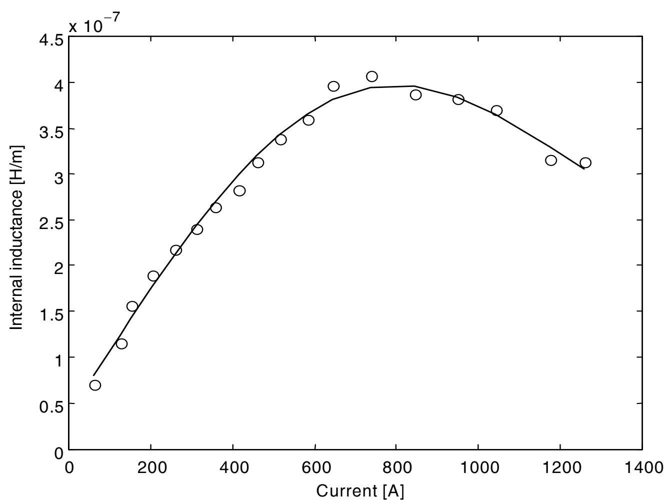

(b)

Figure 10: Per-unit-length rail parameters: (a) R and (b) L_{int} for 1.5 m rail-to-rails separation

TABLE VI

RESULTS FOR 0.5 METRES RAILS SEPARATION

Irms [A]	**R_{rail} [mΩ]**	**L_{tot} [μH]**	**L_{int} [μH]**
123	0.8	8.17	0.99
163.8	0.9	8.26	1.08
197	1.0	8.42	1.24
308.7	1.3	9.31	2.13
394.4	1.6	9.95	2.77
521.7	2.1	10.35	3.17
629.5	2.3	10.27	3.09
733.3	2.5	10.42	3.24
844.5	2.6	10.32	3.14
1010	2.6	10.46	3.28
1119.2	2.5	10.54	3.36
1279.6	2.5	10.46	3.28
1613.8	2.5	9.83	2.65
2092.9	2.4	9.59	2.41

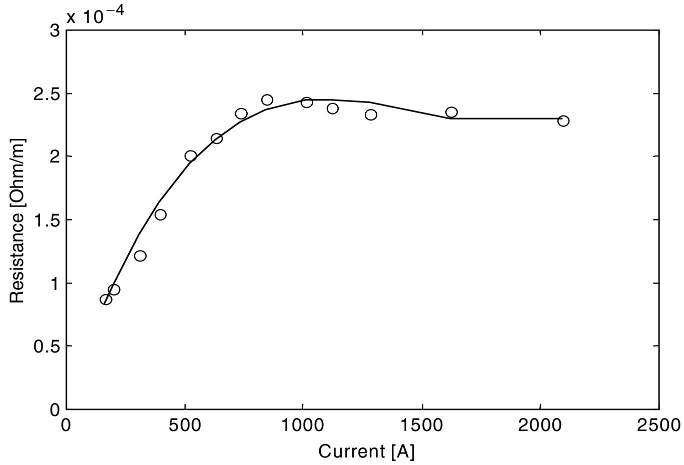

(a)

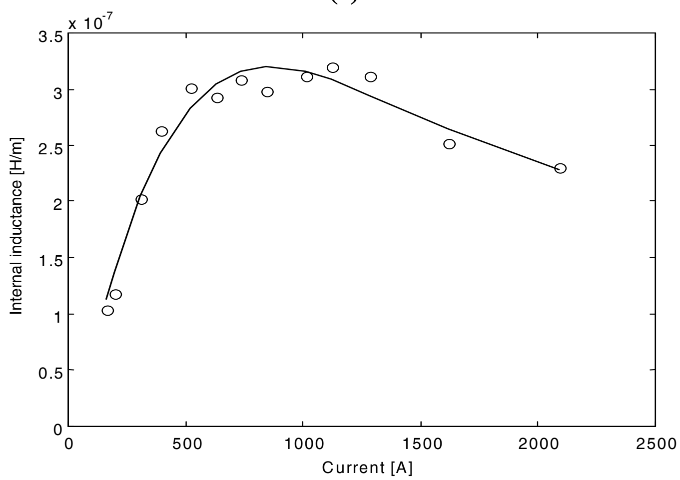

(b)

Figure 11: Per-unit-length rail parameters: (a) R and (b) L_{int} for 0.5 m rail-to-rail separation